Journal of Mathematical Analysis and Applications **252,** 230–255 (2000)
doi:10.1006/jmaa.2000.6994, available online at http://www.idealibrary.com on IDEAL®

Nonlinear Control of Incompressible Fluid Flow: Application to Burgers' Equation and 2D Channel Flow

James Baker, Antonios Armaou, and Panagiotis D. Christofides

Department of Chemical Engineering, University of California, Los Angeles, California 90095-1592
E-mail: pdc@seas.ucla.edu

Submitted by M. J. Balas

Received September 14, 1999

This paper proposes a methodology for the synthesis of nonlinear finite-dimensional feedback controllers for incompressible Newtonian fluid flows described by two-dimensional Navier–Stokes equations. Combination of Galerkin's method with approximate inertial manifolds is employed for the derivation of low-order ordinary differential equation (ODE) systems that accurately describe the dominant dynamics of the flow. These ODE systems are subsequently used as the basis for the synthesis of nonlinear output feedback controllers that guarantee stability and enforce the output of the closed-loop system to follow the reference input asymptotically. The method is successfully used to synthesize nonlinear finite-dimensional output feedback controllers for the Burgers' equation and the two-dimensional channel flow that enhance the convergence rate to the spatially uniform steady-state and the parabolic velocity profile, respectively. The performance of the proposed controllers is successfully tested through simulations and is shown to be superior to the one of linear controllers. © 2000 Academic Press

Key Words: Galerkin's method; approximate inertial manifolds; nonlinear control; Burgers' equation; two-dimensional channel flow.

1. INTRODUCTION

One of the most important problems in the interface of control theory and fluid dynamics is the development of general and practical control methods for systems described by Navier–Stokes equations. The interest on this subject is triggered by a large number of practical applications including feedback control of turbulence for drag reduction, suppression of fluid mechanical instabilities in coating processes, and suppression of instabilities exhibited by falling liquid films, to name a few. For example,

0022-247X/00 $35.00

drag reduction through active feedback control may have a very significant impact on the design and operation of underwater vehicles, airplanes, and automobiles, since according to some estimates keeping the flow over the surface of a vehicle laminar could yield up to 30% reduction in fuel consumption.

The problem of trying to influence a flow field to behave in a desirable way has received significant attention in the past (see, for example, [11, 26–28] for results in this area and reference lists). In general, fluid flow control can be classified in two categories: passive and active. Passive control typically involves some kind of design modification of the surface (e.g., wall-mounted, streamwise ribs, or riblets) and requires no auxiliary power, while active control involves continuous adjustment of a variable that affects the flow based on measurements of quantities of the flow field (feedback). Methods for active fluid flow control include injection of polymers [43, 52], mass transport through porous walls (e.g., blowing/suction) [12, 13], and application of electro-magnetic forcing [19, 46].

The development of an efficient control system for a fluid flow should be based on the specific Navier–Stokes equations that describe the flow in order to exploit their ability to accurately predict the spatiotemporal behavior of the flow field. The main obstacle in following this approach for fluid flow control system design is the infinite-dimensional nature of the Navier–Stokes equations, which prohibits their direct use for the synthesis of practically implementable (low-order) feedback controllers. These controller synthesis and implementation problems, together with the need to develop computationally efficient numerical solution algorithms for the Navier–Stokes equations, have motivated significant research on the understanding of the dynamic behavior of various formulations of the Navier–Stokes equations and the derivation of low-order ODE systems that accurately reproduce their long term dynamics and solutions. The dissipative nature of the Navier–Stokes equations has motivated an extensive research activity on the dynamics where important contributions include the realization that turbulent flows involve coherent structures (e.g., [3, 29]) and their computations [44, 47–49]. The existence of coherent structures implies that the dominant dynamic behavior of transitional and turbulent flows can be approximately described by finite-dimensional systems.

This realization has motivated significant research on the problem of deriving low-order ODE systems that accurately reproduce the dynamics and solutions of fluid flows. An approach to address this problem involves the application of a standard Galerkin's method with empirical eigenfunctions (e.g., [7, 20, 48, 49]) to the Navier–Stokes equations to perform model reduction. Even though this approach has been shown to be very effective,

it does require knowledge of the flow field for a wide range of initial conditions in order to compute the empirical eigenfunctions using Karhunen–Loève expansion, which may not be always available. An alternative approach to low-dimensional modeling of fluid flows is based on the concept of inertial manifold (IM) [50]. If it exists, an IM is a positively invariant, exponentially attracting, finite-dimensional Lipschitz manifold. The IM is an appropriate tools for model reduction because if the trajectories of the Navier–Stokes are on the IM, then this system is exactly described by a low-order ODE system (called inertial form). Unfortunately, even for fluid flows for which an IM is known to exist, the computation of the closed-form expression of the IM (and therefore the derivation of the corresponding inertial form) is a formidable task. Motivated by this, various approaches have been proposed in the literature for the construction of approximations of the inertial manifold (called approximate inertial manifolds (AIMs)) (see, for example, [16, 22, 23]). The AIMs are subsequently used for the derivation of approximations of the inertial form that accurately reproduce the solutions and dynamics of the flow field. The combination of Galerkin's method with AIMs leads to a nonlinear Galerkin's method (e.g., [24, 35, 45, 51]). Finally, another approach to low-dimensional modeling of fluid flows is based on the reduced basis methods (e.g., [35, 36]).

On the other hand, research on control of Navier–Stokes equations has mainly focused on the use of proportional-integral control [8, 13, 14, 39], linear optimal control [21, 32, 34, 38], H_∞ optimal control [9, 10, 17, 18, 41], and Lyapunov-based control [40] to regulate various fluid flows. At this stage, not much work has been done on the utilization of nonlinear model reduction techniques for the design of nonlinear low-order feedback controllers for fluid flows with well-characterized closed-loop stability, performance, and robustness properties.

In this work, we focus on nonlinear control of incompressible Newtonian fluid flows described by two-dimensional Navier–Stokes equations. Initially, a nonlinear Galerkin's method is used to derive low-dimensional ODE models, which are subsequently used for the synthesis of low-order nonlinear output feedback controllers that enforce the desired stability properties in the closed loop system. The method is successfully used to synthesize nonlinear finite-dimensional output feedback controllers for the Burgers' equation and the two-dimensional channel flow that enhance the convergence rates to the spatially uniform steady-state and the parabolic velocity profile, respectively. The performance of the proposed controllers is successfully tested through simulations and is shown to be superior to the one of linear controllers.

2. THE 2D NAVIER–STOKES EQUATIONS: PRELIMINARIES

We consider incompressible two-dimensional Newtonian fluid flows which are described by the Navier–Stokes equations,

$$\begin{aligned} \frac{\partial U}{\partial t} + (U \cdot \nabla)U &= -\frac{\nabla P}{\rho} + \nu \nabla^2 U + wb(z)u(t) \\ \nabla \cdot U &= 0 \\ y_m(t) = \int_\Omega s(z)U\,dz, &\qquad y_c(t) = \int_\Omega c(z)U\,dz \end{aligned} \tag{1}$$

subject to the boundary and initial conditions:

$$U = 0 \text{ on } \Gamma, \qquad U(z,t) = U_0, \tag{2}$$

where Ω is the two-dimensional domain, Γ is the boundary of Ω, $z = [z_1 \;\; z_2]^T$ is the spatial coordinate, $U(z,t) = [U_1(z,t) \;\; U_2(z,t)]^T$ is the velocity vector, $P(z,t)$ is the pressure, ν is the (constant) kinematic viscosity, ρ is the (constant) density, $u(t) = [u_1(t) \cdots u_l(t)] \in \mathbb{R}^l$ is the vector of manipulated inputs, $y_m(t) = [y_{m_1} \cdots y_{m_q}] \in \mathbb{R}^q$ is the vector of measured outputs, $y_c(t) = [y_{c_1} \cdots y_{c_l}] \in \mathbb{R}^l$ is the vector of controlled outputs, w is a constant vector, $b(z) = [b^1(z) \cdots b^l(z)]$ is the vector of actuator distribution functions (i.e., $b^i(z)$ describes how the control action $u_i(t)$ is distributed on Ω), $s(z)$ is a vector function which depends on the characteristics of the measurement sensors (e.g., point/distributed sensing), and $c(z)$ is a vector function which depends on the performance specifications. Whenever the control action enters the system at a single point z_0, with $z_0 \in \Omega$ (i.e., point actuation, where $b(z) = \delta(z - z_0)$; $\delta(\cdot)$ denotes the dirac function), the function $b(z)$ is taken to be nonzero in a finite spatial interval of the form $[z_0 - \epsilon, z_0 + \epsilon]$, where ϵ is a small positive real number, and zero elsewhere in Ω.

We formulate the Navier–Stokes equations (Eqs. (1)–(2)) as an infinite-dimensional system in the Hilbert space $\mathscr{H} = \{U \in L^2(\Omega)^2 \mid \nabla \cdot U = 0, U = 0 \text{ on } \Gamma\}$ (i.e., $\mathscr{H}$ is a space of two-dimensional vector functions defined on Ω that satisfy the boundary condition of Eq. (2) and $\nabla \cdot U = 0$), with inner product and norm

$$(\omega_1, \omega_2) = \int_\Omega (\omega_1(z), \omega_2(z))_{\mathbb{R}^2}\,dz, \qquad \|\omega_1\|_2 = (\omega_1, \omega_1)^{1/2}, \tag{3}$$

where ω_1, ω_2 are two elements of $\mathscr{H}$ and the notation $(\cdot,\cdot)_{\mathbb{R}^2}$ denotes the

standard inner product in $\mathbb{R}^2$. Defining the state function x on $\mathscr{H}$ as

$$x(t) = U(z,t), \qquad t > 0,\ z \in \Omega, \tag{4}$$

and the orthogonal L^2 projection $\Pi : L^2(\Omega)^2 \to \mathscr{H}$, projecting the Navier–Stokes equations into $\mathscr{H}$ and defining

$$\begin{gathered} \mathscr{A}x = \Pi\,\nabla^2 U, \qquad \mathscr{B}u = \Pi wbu, \qquad \mathscr{R}(x) = \Pi\big[(U\cdot\nabla)U\big], \\ \mathscr{S}x = (s,x), \qquad \mathscr{C}x = (c,x) \end{gathered} \tag{5}$$

we obtain the following representation of the Navier–Stokes equations in $\mathscr{H}$,

$$\begin{gathered} \dot{x} = \nu\mathscr{A}x + \mathscr{B}u + \mathscr{R}(x), \qquad x(0) = x_0 \\ y_m = \mathscr{S}x, \qquad y_c = \mathscr{C}x. \end{gathered} \tag{6}$$

In the above system $\mathscr{A} : D(\mathscr{A}) \subset \mathscr{H} \to \mathscr{H}$ is a densely defined, unbounded, self-adjoint, and positive operator with compact inverse which includes all the higher-order spatial derivatives and $\mathscr{R} : D(\mathscr{R}) \subset \mathscr{H} \to \mathscr{H}$ is a nonlinear map which gathers low order spatial derivatives and nonlinear terms.

For $\mathscr{A}$, the eigenvalue problem is defined as

$$\mathscr{A}\phi_j = \lambda_j \phi_j, \qquad j = 1, \ldots, \infty, \tag{7}$$

where λ_j and ϕ_j denote the jth eigenvalue and eigenfunction, respectively; the eigenspectrum of $\mathscr{A}$, $\sigma(\mathscr{A})$, is defined as the set of all eigenvalues of $\mathscr{A}$, i.e., $\sigma(\mathscr{A}) = \{\lambda_1, \lambda_2, \ldots\}$. The eigenvalues of $\mathscr{A}$ satisfy $0 > \lambda_1 \geq \lambda_2 \geq \cdots$ while the eigenfunctions $\{\phi_1, \phi_2, \ldots\}$ form a complete orthonormal set in $\mathscr{H}$ (e.g., [50]).

Finally, we recall the Lie derivative notion which will be used in our development: $L_f h$ denotes the Lie derivative of a scalar field h with respect to the vector field f, $L_f^k h$ denotes the kth order Lie derivative, and $L_g L_f^{k-1} h$ denotes the mixed Lie derivative.

Remark 1. We note that in most practical cases the computation of the eigenfunctions of $\mathscr{A}$ is a very difficult task, and thus, one may have to use appropriate sets of basis functions which are defined in $\mathscr{H}$ (see, for example, the channel flow problem considered in Section 6) or compute empirical eigenfunctions of the system of Eq. (6) through Karhunen–Loève expansion (known also as proper orthogonal decomposition); the reader may refer to [25, 31] for a general presentation and analysis of the Karhunen–Loève expansion and to [2] for results of finite-dimensional approximation and control of nonlinear parabolic PDEs using empirical eigenfunctions.

3. NONLINEAR MODEL REDUCTION

We apply a nonlinear Galerkin's method [7, 20, 51] to the system of Eq. (6) to derive an approximate finite-dimensional system. Let $\mathscr{H}_s, \mathscr{H}_f$ be modal subspaces of $\mathscr{H}$, defined as $\mathscr{H}_s = span\{\phi_1, \phi_2, \ldots, \phi_m\}$ and $\mathscr{H}_f = span\{\phi_{m+1}, \phi_{m+2}, \ldots\}$. Clearly, $\mathscr{H}_s \oplus \mathscr{H}_f = \mathscr{H}$. Defining the orthogonal projection operators $P_s : \mathscr{H} \to \mathscr{H}_s$ and $P_f : \mathscr{H} \to \mathscr{H}_f$ such that $x_s = P_s x$, $x_f = P_f x$, the state x of the system of Eq. (6) can be decomposed to

$$x = x_s + x_f = P_s x + P_f x. \tag{8}$$

Applying P_s and P_f to the system of Eq. (6) and using the above decomposition for x, the system of Eq. (6) can be written in the form

$$\begin{aligned}
\frac{dx_s}{dt} &= \nu \mathscr{A}_s x_s + \nu \mathscr{A}_{sf} x_f + \mathscr{B}_s u + \mathscr{R}_s(x_s, x_f), \qquad x_s \in \mathscr{H}_s \\
\frac{\partial x_f}{\partial t} &= \nu \mathscr{A}_{fs} x_s + \nu \mathscr{A}_f x_f + \mathscr{B}_f u + \mathscr{R}_f(x_s, x_f), \qquad x_f \in \mathscr{H}_f \\
y_m &= \mathscr{S} x_s + \mathscr{S} x_f, \qquad y_c = \mathscr{C} x_s + \mathscr{C} x_f \\
x_s(0) &= P_s x(0) = P_s x_0, \qquad x_f(0) = P_f x(0) = P_f x_0,
\end{aligned} \tag{9}$$

where $\mathscr{A}_s x_s + \mathscr{A}_{sf} x_f = P_s \mathscr{A} x$, $\mathscr{B}_s = P_s \mathscr{B}$, $\mathscr{R}_s = P_s \mathscr{R}$, $\mathscr{A}_{fs} x_s + \mathscr{A}_f x_f = P_f \mathscr{A} x$, $\mathscr{B}_f = P_f \mathscr{B}$, and $\mathscr{R}_f = P_f \mathscr{R}$ and the notation $\partial x_f / \partial t$ is used to denote that the state x_f belongs to an infinite-dimensional space. In the above system, $\mathscr{A}_s$ is a matrix of dimension $m \times m$, $\mathscr{R}_s(x_s, x_f)$ and $\mathscr{R}_f(x_s, x_f)$ are Lipschitz vector functions, and $\mathscr{A}_f$ is a stable unbounded differential operator. Referring to the system of Eq. (9), we note that the presence of the linear terms $\mathscr{A}_{sf} x_f$, $\mathscr{A}_{fs} x_s$ is due to the fact that we have not restricted $\mathscr{H}_s$ and $\mathscr{H}_f$ to be modal subspaces spanned by the eigenfunctions of $\mathscr{A}$. This is in contrast to our previous work in [1] where $\mathscr{H}_s$ and $\mathscr{H}_f$ were assumed to be modal subspaces spanned by the eigenfunctions of $\mathscr{A}$ and introduces additional complications in the solution of the control problem (see condition (4) in Theorem 1 and Remarks 4 and 5 below).

The standard Galerkin's method is to approximate the solution $x(t)$ of the system of Eq. (6) by $\bar{x}_s \in \mathscr{H}_s$ which is given by the m-dimensional system

$$\begin{aligned}
\frac{d\bar{x}_s}{dt} &= \nu \mathscr{A}_s \bar{x}_s + \mathscr{B}_s u + \mathscr{R}_s(\bar{x}_s, 0) \\
y_m &= \mathscr{S} \bar{x}_s, \qquad y_c = \mathscr{C} \bar{x}_s.
\end{aligned} \tag{10}$$

A finite-dimensional system of order m which yields solutions which are closer to the one of the system of Eq. (6) than the ones obtained by the system of Eq. (10) can be obtained by using the concept of inertial manifold (IM). If it exists, an inertial manifold $\mathcal{M}$ for the system of Eq. (6) is a subset of $\mathcal{H}$, which satisfies the following properties [50]: (i) $\mathcal{M}$ is a finite-dimensional Lipschitz manifold, (ii) $\mathcal{M}$ is a graph of a Lipschitz function $\Sigma(x_s, u)$ mapping $\mathcal{H}_s \times \mathbb{R}^l$ onto $\mathcal{H}_f$ and for every solution $x_s(t), x_f(t)$ of Eq. (9) with $x_f(0) = \Sigma(x_s(0), u)$, then

$$x_f(t) = \Sigma\big(x_s(t), u\big), \qquad \forall t \geq 0, \tag{11}$$

and (iii) $\mathcal{M}$ attracts every trajectory exponentially. The evolution of the state x_f on $\mathcal{M}$ is given by Eq. (11), while the evolution of the state x_s is governed by the finite-dimensional inertial form

$$\begin{aligned} \frac{d\tilde{x}_s}{dt} &= \nu\mathcal{A}_s\tilde{x}_s + \nu\mathcal{A}_{sf}\Sigma\big(\tilde{x}_s, u\big) + \mathcal{B}_s u + \mathcal{R}_s\big(\tilde{x}_s, \Sigma\big(\tilde{x}_s, u\big)\big) \\ y_m &= \mathcal{S}x_s + \mathcal{S}\Sigma\big(\tilde{x}_s, u\big) \\ y_c &= \mathcal{C}x_s + \mathcal{C}\Sigma\big(\tilde{x}_s, u\big), \end{aligned} \tag{12}$$

where $\tilde{x}_s$ denotes the solution of the x_s subsystem on $\mathcal{M}$. Assuming that $u(t)$ is smooth, differentiating Eq. (11) and utilizing Eq. (9), $\Sigma(x_s, u)$ can be computed as the solution of the partial differential equation

$$\begin{aligned} &\frac{\partial\Sigma}{\partial x_s}\Big[\nu\mathcal{A}_s x_s + \nu\mathcal{A}_{sf}\Sigma\big(\tilde{x}_s, u\big) + \mathcal{B}_s u + \mathcal{R}_s\big(x_s, \Sigma\big(x_s, u\big)\big)\Big] + \frac{\partial\Sigma}{\partial u}\dot{u} \\ &\quad = \nu\mathcal{A}_{fs}x_s + \nu\mathcal{A}_f\Sigma\big(x_s, u\big) + \mathcal{B}_f u + \mathcal{R}_f\big(x_s, \Sigma\big(x_s, u\big)\big) \end{aligned} \tag{13}$$

which $\Sigma(x_s, u)$ has to satisfy for all $x_s \in \mathcal{H}_s$, $u \in \mathbb{R}^l$. Unfortunately, even for PDEs for which an IM is known to exist, the derivation of an explicit analytic form of $\Sigma(x_s, u)$ is an almost impossible task. The nonlinear Galerkin method attempts to overcome the problems associated with the construction of inertial manifolds by replacing $\Sigma(\tilde{x}_s, u)$ with an approximate relation $\Sigma_{app}(\tilde{x}_s, u)$ (called approximate inertial manifold (AIM)). In this case, the solution x of the system of Eq. (6) is approximated by $\tilde{x}_s + \Sigma_{app}(\tilde{x}_s, u)$ which is given by the m-dimensional system

$$\begin{aligned} \frac{d\tilde{x}_s}{dt} &= \nu\mathcal{A}_s\tilde{x}_s + \nu\mathcal{A}_{sf}\Sigma_{app}\big(\tilde{x}_s, u\big) + \mathcal{B}_s u + \mathcal{R}_s\big(\tilde{x}_s, \Sigma_{app}\big(\tilde{x}_s, u\big)\big) \\ y_m &= \mathcal{S}\tilde{x}_s + \mathcal{S}\Sigma_{app}\big(\tilde{x}_s, u\big) \\ y_c &= \mathcal{C}\tilde{x}_s + \mathcal{C}\Sigma_{app}\big(\tilde{x}_s, u\big). \end{aligned} \tag{14}$$

To construct $\Sigma_{app}(\tilde{x}_s, u)$, we take advantage of the fact that the dynamics of the x_f subsystem are stable and faster than the ones of the x_s modes (note that the number of unstable eigenvalues of the system of Eq. (6) is finite, and by construction of $\mathscr{H}_s$ and $\mathscr{H}_f$, all the unstable eigenvalues are included in the x_s subsystem) and compute $\Sigma_{app}(\tilde{x}_s, u)$ by setting $\dot{x}_f = \nu\mathscr{A}_{fs}\tilde{x}_s + \nu\mathscr{A}_f\Sigma + \mathscr{B}_f u + \mathscr{R}_f(\tilde{x}_s, \Sigma) \equiv 0$ and solving the equation

$$\nu\mathscr{A}_{fs}\tilde{x}_s + \nu\mathscr{A}_f\Sigma + \mathscr{B}_f u + \mathscr{R}_f(\tilde{x}_s, \Sigma) = 0. \tag{15}$$

This can be accomplished by using a standard successive approximation (fixed point) algorithm [24] (see also [45]),

$$\begin{aligned} \Sigma_{app_{\zeta+1}}(\tilde{x}_s, u) &= -(\nu\mathscr{A}_f)^{-1}\left[\nu\mathscr{A}_{fs}\tilde{x}_s + \mathscr{B}_f u + \mathscr{R}_f\left(\tilde{x}_s, \Sigma_{app_\zeta}\right)\right], \\ &\qquad \zeta = 0, \ldots, \kappa - 1, \ \Sigma_{app_0}(\tilde{x}_s, u) = 0 \\ \tilde{x}_f &= \Sigma_{app_\kappa}(\tilde{x}_s, u), \end{aligned} \tag{16}$$

where $\Sigma_{app_\kappa}(\tilde{x}_s, u)$ is the resulting approximation of $\Sigma(\tilde{x}_s, u)$ and $\tilde{x}_f$ is the approximation of x_f. When $\zeta = 0$, the following approximation of $\Sigma(\tilde{x}_s, u)$, which is frequently used in the literature (see, for example, [37]) and does not require a recursive algorithm, is obtained:

$$\Sigma_{app_1}(\tilde{x}_s, u) = -(\nu\mathscr{A}_f)^{-1}\left[\nu\mathscr{A}_{fs}\tilde{x}_s + \mathscr{B}_f u + \mathscr{R}_f(\tilde{x}_s, 0)\right]. \tag{17}$$

Substituting the approximation of the inertial manifold of Eq. (16) into the m-dimensional system of Eq. (12), we obtain the following system which can be used for controller design:

$$\begin{aligned} \frac{d\tilde{x}_s}{dt} &= \nu\mathscr{A}_s\tilde{x}_s + \nu\mathscr{A}_{sf}\Sigma_{app_\kappa}(\tilde{x}_s, u) + \mathscr{B}_s u + \mathscr{R}_s\left(\tilde{x}_s, \Sigma_{app_\kappa}(\tilde{x}_s, u)\right) \\ y_m &= \mathscr{S}x_s + \mathscr{S}\Sigma_{app_\kappa}(\tilde{x}_s, u) \\ y_c &= \mathscr{C}x_s + \mathscr{C}\Sigma_{app_\kappa}(\tilde{x}_s, u). \end{aligned} \tag{18}$$

Remark 2. We note that even though many fluid flows exhibit low-dimensional dynamic behavior, the delicate mathematical question of rigorously establishing existence of inertial manifolds for fluid flow models, at this stage, is unresolved. Such a question has been positively answered for certain classes of diffusion-reaction systems and the Kuramoto–Sivashinsky equation (see [50] for details).

Remark 3. The expression of the approximate inertial manifold $\Sigma_{app_\kappa}(\tilde{x}_s, u)$ of Eq. (16) (where κ is chosen based on the desired degree of approximation) was originally proposed in [24] and is called the steady

manifold. The reader may also refer to [16, 24, 45] for alternative expressions of $\Sigma_{app}(\tilde{x}_s, u)$, as well as detailed computational studies that show that the use of approximate inertial manifolds leads to accurate low-order ODE approximations and low-order controllers for diffusion-reaction systems described by parabolic partial differential equations.

4. NONLINEAR CONTROL

In this section, we use the system of Eq. (18) to synthesize a nonlinear finite-dimensional output feedback controller through combination of a state feedback controller with a state observer. We then derive precise conditions (see Theorem 1 below) which ensure that this controller guarantees stability and enforces output tracking in the closed-loop infinite-dimensional system. Motivated by the nonlinear appearance of the manipulated input in the system of Eq. (18) and following the development in [1], we initially implement the following preliminary dynamic feedback law,

$$\begin{aligned} \frac{d\xi}{dt} &= \bar{u} \\ u &= \xi, \end{aligned} \tag{19}$$

where $\bar{u}$ is an auxiliary input, on the system of Eq. (18) to obtain

$$\begin{aligned} \frac{d\xi}{dt} &= \bar{u} \\ \frac{d\tilde{x}_s}{dt} &= \nu\mathscr{A}_s\tilde{x}_s + \nu\mathscr{A}_{sf}\Sigma_{app_\kappa}(\tilde{x}_s, \xi) + \mathscr{B}_s\xi + \mathscr{R}_s\big(\tilde{x}_s, \Sigma_{app_\kappa}(\tilde{x}_s, \xi)\big) \\ y_m &= \mathscr{S}\tilde{x}_s + \mathscr{S}\Sigma_{app_\kappa}(\tilde{x}_s, \xi) \\ y_c &= \mathscr{C}\tilde{x}_s + \mathscr{C}\Sigma_{app_\kappa}(\tilde{x}_s, \xi) \end{aligned} \tag{20}$$

which can be written in the compact form

$$\begin{aligned} \frac{d\hat{x}_s}{dt} &= f(\hat{x}_s) + g(\hat{x}_s)\bar{u} \\ y_m &= h_m(\hat{x}_s), \qquad y_c = h_c(\hat{x}_s), \end{aligned} \tag{21}$$

where $\hat{x}_s = [\xi^T \ \tilde{x}_s^T]^T$ and the specific form of f, g, h_m, h_c can be readily obtained by comparing Eq. (20) and Eq. (21). On the basis of the system of Eq. (21), one can utilize geometric control methods [33] to synthesize a

nonlinear state feedback control law of the general form

$$\bar{u} = p(\hat{x}_s) + Q(\hat{x}_s)v, \tag{22}$$

where $p(\hat{x}_s)$ is a smooth vector function, $Q(\hat{x}_s)$ is a smooth matrix, and $v \in \mathbb{R}^l$ is the constant reference input vector. Under the hypothesis that the system of Eq. (21) is locally observable (i.e., its linearization around the zero solution is observable), the practical implementation of the state feedback law of Eq. (22) will be achieved by employing the nonlinear state observer,

$$\frac{d\eta}{dt} = f(\eta) + g(\eta)\bar{u} + L(y_m - h_m(\eta)), \tag{23}$$

where η denotes the observer state vector (the dimension of the vector η is equal to the dimension of $\hat{x}_s$ in the system of Eq. (21)), and L is a matrix chosen so that the eigenvalues of the matrix $C_L = (\partial f/\partial\eta)|_{(\eta=0)} - L(\partial h_m/\partial\eta)|_{(\eta=0)}$ lie in the open left-hand of the complex plane.

The dynamic control law of Eq. (19), the state feedback law of Eq. (22), and the state observer of Eq. (23) can be combined to yield the following nonlinear output feedback controller:

$$\begin{aligned} \frac{d\eta}{dt} &= f(\eta) + g(\eta)(p(\eta) + Q(\eta)v) + L(y_m - h_m(\eta)) \\ u &= \hat{\xi}, \end{aligned} \tag{24}$$

where $\hat{\xi}$ is the estimate for ξ which is obtained by the state observer of Eq. (23). Theorem 1 below provides an explicit synthesis formula of the output feedback controller and conditions that guarantee closed-loop stability. In order to state the result of the theorem, referring to the system of Eq. (21), we define the relative order of the output y_{c_i} with respect to the vector of manipulated inputs $\bar{u}$ as the smallest integer r_i for which

$$\left[L_{g_1}L_f^{r_i-1}h_{c_i}(\hat{x}_s) \cdots L_{g_l}L_f^{r_i-1}h_{c_i}(\hat{x}_s)\right] \not\equiv [0 \cdots 0] \tag{25}$$

or $r_i = \infty$ if such an integer does not exist, and the characteristic matrix

$$C(\hat{x}_s) = \begin{bmatrix} L_{g_1}L_f^{r_1-1}h_{c1}(\hat{x}_s) & \cdots & L_{g_l}L_f^{r_1-1}h_{c1}(\hat{x}_s) \\ L_{g_1}L_f^{r_2-1}h_{c2}(\hat{x}_s) & \cdots & L_{g_l}L_f^{r_2-1}h_{c2}(\hat{x}_s) \\ \vdots & \cdots & \vdots \\ L_{g_1}L_f^{r_l-1}h_{cl}(\hat{x}_s) & \cdots & L_{g_l}L_f^{r_l-1}h_{cl}(\hat{x}_s) \end{bmatrix}, \tag{26}$$

where h_{ci} is the ith element of the vector h_c and g_i is the ith vector of the matrix g.

THEOREM 1. *Consider the system of Eq.* (21) *and assume that*: (1) *it is locally observable and* $C_L = (1/\epsilon)A$ *where* ϵ *is a small positive parameter and* A *is a Hurwitz matrix*, (2) *its characteristic matrix is nonsingular* $\forall\ \hat{x}_s$, (3) *its unforced* ($v \equiv 0$) *zero dynamics are locally exponentially stable, and* (4) *the matrix* $A_{cl} = \begin{bmatrix} \hat{\mathscr{A}}_s + \hat{\mathscr{B}}_s F & \hat{\mathscr{A}}_{sf} \\ \hat{\mathscr{A}}_{fs} & \hat{\mathscr{A}}_f \end{bmatrix}$ *where all the elements are defined in the proof, is stable. Consider also the system of Eq.* (6) *under the nonlinear output feedback controller*,

$$\frac{d\eta}{dt} = f(\eta) + L(y_m - h_m(\eta)) + g(\eta)\left\{\left[\beta_{1r_1} \cdots \beta_{lr_l}\right]C(\eta)\right\}^{-1}\left\{v - \sum_{i=1}^{l}\sum_{k=0}^{r_i}\beta_{ik}L_f^k h_{ci}(\eta)\right\} \quad (27)$$

$$u = \hat{\xi},$$

where the l-dimensional vectors of the parameters β_{ik} *are chosen so that the roots of the equation* $\det(B(s)) = 0$ *are in the open left-half of the complex plane* ($B(s)$ *is a* $l \times l$ *matrix, whose* (i, j)*th element is of the form* $\sum_{k=0}^{r_i}\beta_{jk}^i s^k$). *Then, there exist positive real numbers* μ, ϵ^* *such that if* $\|x_0\|_2 \le \mu$ *and* $\epsilon \in (0, \epsilon^*]$, *the zero solution of the closed-loop system* (*Eqs.* (6) *and* (27)) *is exponentially stable.*

Remark 4. The assumption that the zero dynamics of the system of Eq. (21) are locally exponentially stable is standard in geometric control (see [33] for details), while the assumption $C_L = (1/\epsilon)A$, where ϵ is a small positive parameter and A is a Hurwitz matrix, is needed to ensure that the presence of closed-loop system states, which are not included in the model used for controller synthesis, in the state observer do not lead to closed-loop instability. Finally, the assumption that the characteristic matrix $C(\hat{x}_s)$ is nonsingular is made to simplify the presentation of the controller synthesis results and can be relaxed (see [33]), while the requirement on matrix A_{cl} is needed because $\mathscr{H}_s$ and $\mathscr{H}_f$ are assumed to be modal subspaces of $\mathscr{H}$ and can be relaxed when $\mathscr{H}_s$ and $\mathscr{H}_f$ are assumed to be modal subspaces spanned by the eigenfunctions of $\mathscr{A}$.

Remark 5. The requirement on matrix A_{cl} depends on the structure of the matrices $\hat{\mathscr{B}}_s, \hat{\mathscr{B}}_f$, and therefore, on the shape of the actuator distribu-

tion functions b_i which, in most practical applications, cannot be chosen by the control designer. Whenever the requirement on matrix A_{cl} is not satisfied, one can use more control actuators to ensure the stability of the closed-loop system via state feedback. Finally, even though the matrix A_{cl} has infinite range, the fact that the eigenvalues of the operator $\mathscr{A}$ grow towards negative infinity implies that the verification of the stability of A_{cl} can be done on the basis of a sufficiently large finite-dimensional approximation of the closed-loop system (this fact is numerically verified in Section 6 in the channel flow problem).

Remark 6. The implementation of the controller of Eq. (27) requires us to explicitly compute the vector function $\Sigma_{app}(\eta, u)$. However, $\Sigma_{app}(\eta, u)$ has an infinite-dimensional range and therefore cannot be implemented in practice. Instead a finite-dimensional approximation of $\Sigma_{app}(\eta, u)$, say $\Sigma_{app_t}(\eta, u)$, can be derived by keeping the first $\tilde{m}$ elements of $\Sigma_{app}(\eta, u)$ and neglecting the remaining infinite ones. Clearly, as $\tilde{m} \to \infty$, $\Sigma_{app_t}(\eta, u)$ approaches $\Sigma_{app}(\eta, u)$. This implies that by picking $\tilde{m}$ to be sufficiently large, the controller of Eq. (27) with $\Sigma_{app_t}(\eta, u)$ instead of $\Sigma_{app}(\eta, u)$ enforces local exponential stability in the closed-loop infinite-dimensional system.

Remark 7. An approximate way to deal with the nonlinear appearance of the manipulated input u in the system of Eq. (18) without having to employ dynamic state feedback is to design a control law, say u_0, on the basis of the finite-dimensional model obtained from the standard Galerkin's method where the input enters linearly (Eq. (10)), and then design, the state feedback controller on the basis of the system of Eq. (18) with $\Sigma_{app_\kappa}(\tilde{x}_s, u_0)$. This approach is suitable for parabolic-like infinite dimensional systems (see Section 5 below for an application of this technique to the Burgers' equation) and is motivated by the highly dissipative nature of such systems (see also [4–6, 15] for additional results on control of parabolic PDEs).

5. NONLINEAR FINITE-DIMENSIONAL CONTROL OF BURGER'S EQUATION

We consider the one-dimensional Burgers' equation with distributed control,

$$\frac{\partial U}{\partial t} = \frac{1}{Re}\frac{\partial^2 U}{\partial z^2} - U\frac{\partial U}{\partial z} + b(z)u(t) \tag{28}$$

subject to the Dirichlet boundary conditions,

$$U(0,t) = 0, \qquad U(\pi,t) = 0 \tag{29}$$

and the initial condition

$$U(z,0) = U_0(z), \tag{30}$$

where U denotes the dimensionless velocity in the axial direction, Re is the Reynolds number, u denotes the manipulated input, and $b(z)$ is the actuator distribution function. For the system of Eq. (28), the spatiotemporal evolution of the open-loop velocity, for $Re = 200$ and $U_0(z) = 1.5\sum_{m=1}^{2} \sin(m, z)$, is shown in Fig. 1. The open-loop system was solved by using Galerkin's method with one hundred eigenfunctions of the spatial operator (see Eq. (32) below); further increase on the number of eigenfunctions does not change the accuracy of the results. It is clear that for this value of the Reynolds number, the time required for the velocity profile to approach the stable zero solution is significant (i.e., more than 30 time units). Moreover, $U(z,t)$ exhibits a sharp maximum close to the wall (this is because, for $Re = 200$, the contribution of the convective term, $U(\partial U/\partial z)$, is important). We use the methodology presented in the paper to design a nonlinear finite-dimensional controller which uses a single velocity measurement at $z = \frac{\pi}{2}$ (i.e., $s(z) = \delta(z - \frac{\pi}{2})$) to accelerate the

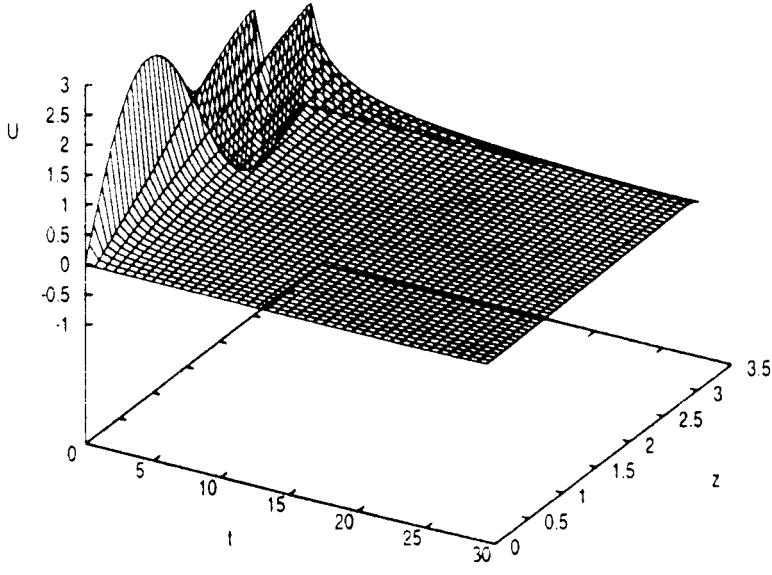

FIG. 1. Profile of evolution of open-loop velocity—Burgers' equation.

convergence of the initial state $U_0(z) = 1.5\sum_{m=1}^{2} \sin(m\ z)$ to zero, while smoothening the sharp transient behavior. To achieve this control objective, the controlled output was defined as

$$y_c(t) = \int_0^{\pi} \sqrt{\frac{2}{\pi}}\ \sin(z) U(z,t)\ dz \tag{31}$$

and the actuator distribution function was taken to be $b(z) = \exp(-1.5z)$ (this kind of actuator distribution function can be achieved in practice when electromagnetic Lorenz forces are applied to the flow near the bottom wall [19, 46]). The eigenvalue problem for the linear spatial differential operator of the system of Eq. (28), $\partial^2 U/\partial z^2$, subject to the Dirichlet boundary condition, can be solved analytically and its solution is of the form

$$\lambda_j = -j^2, \qquad \phi_j(z) = \sqrt{\frac{2}{\pi}}\ \sin(j\quad z), \qquad j = 1, \ldots, \infty. \tag{32}$$

For the system of Eq. (28), Galerkin's method with approximate inertial manifolds was used to derive an approximate eight-dimensional ODE model which uses a 12th-order approximation for the approximate inertial manifold (i.e., $m = 8$ and $\bar{m} = 12$); this ODE model was employed for controller design. No improvement on the accuracy of the AIM through the iterative scheme of Eq. (16) was used. The controller was synthesized by using the approximate scheme discussed in Remark 7 and the formula of Eq. (27), and was implemented in the simulations with

$$\beta_{10} = \begin{bmatrix} 2.0 \\ 0.0 \\ \vdots \\ 0.0 \end{bmatrix}, \qquad \beta_{11} = \begin{bmatrix} 1.0 \\ 0.0 \\ \vdots \\ 0.0 \end{bmatrix}, \qquad \text{and} \qquad L = \begin{bmatrix} -5.0 \\ 2.0 \\ 0.0 \\ \vdots \\ 0.0 \end{bmatrix}.$$

Figures 2, 3, and 4 (dashed line) show the evolution of the velocity profile, the manipulated input profile, and the energy of the closed-loop system under the nonlinear controller; the initial condition is

$$U_0(z) = 1.5 \sum_{m=1}^{2} \sin(m\quad z).$$

Clearly, the nonlinear controller drives $U(z,t)$ faster to zero (compare the energy of the open-loop system (solid line) and the closed-loop system in Fig. 4), while achieving a smooth transient profile. For the sake of

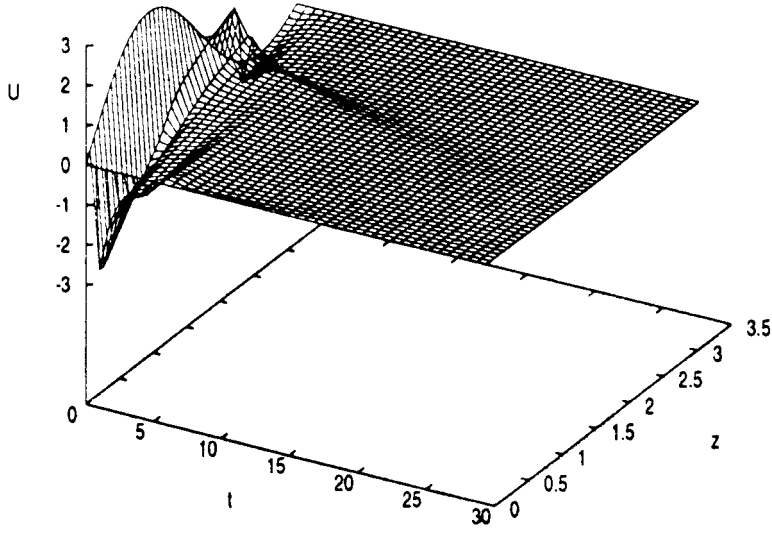

FIG. 2. Closed-loop velocity profile under nonlinear control—Burgers' equation.

comparison, we also implemented on Burgers' equation a linear controller obtained from the Taylor linearization of the nonlinear controller around the steady state $U(z, t) = 0$. Figure 4 (dotted line) shows the energy of the closed-loop system under the linear controller. It is clear that the nonlinear controller drives the energy of the closed-loop system to zero faster than the linear one, thereby establishing the superiority of nonlinear control (note that the order of the two controllers is the same (8)).

6. NONLINEAR FINITE-DIMENSIONAL CONTROL OF 2D CHANNEL FLOW

In this section, we use the proposed method to synthesize a nonlinear feedback controller for the two-dimensional channel flow. The control objective is to enhance the convergence rate to the steady-state parabolic velocity profile, and the control actuation is assumed to be in the form of electromagnetic Lorenz forces applied to the flow near the bottom wall [19, 46] (see Fig. 5 for a schematic of the flow). To present the various equations that describe the flow, we use the characteristic time $t = h/U_c$ where h is the half-channel height and U_c is the center-channel velocity, as well as the Reynolds number $Re = U_c h/\nu$ where ν is the kinematic viscosity. In two dimensions, the continuity and Navier–Stokes equations

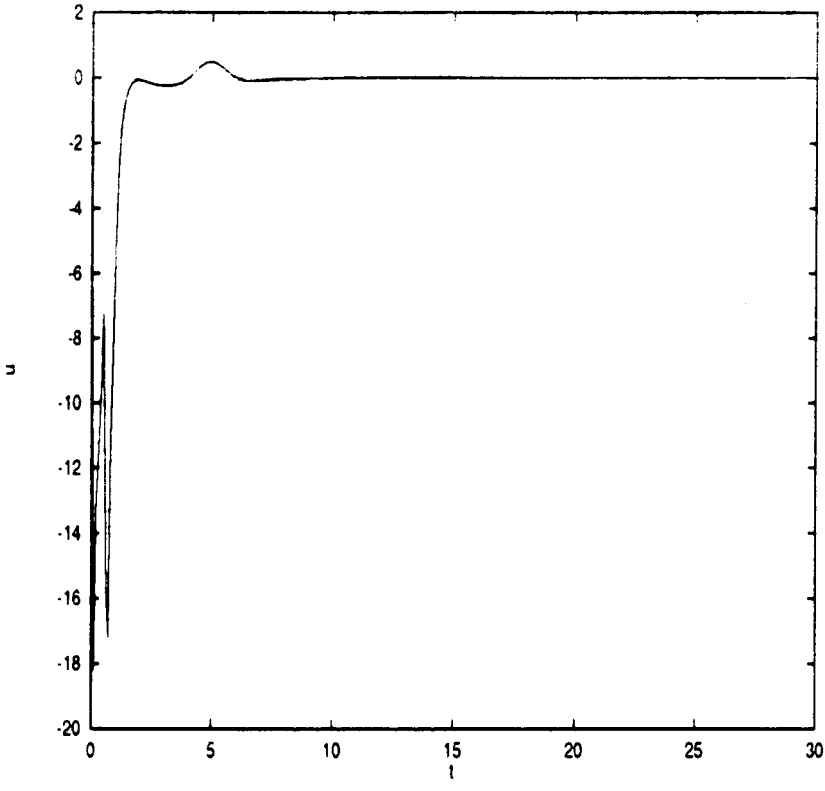

FIG. 3. Manipulated input profile for nonlinear controller—Burgers' equation.

take the form

$$\frac{\partial u^*}{\partial x} + \frac{\partial v^*}{\partial y} = 0, \tag{33}$$

$$\begin{aligned}\frac{\partial u^*}{\partial t} + u^*\frac{\partial u^*}{\partial x} + v^*\frac{\partial u^*}{\partial y} &= -\frac{\partial p^*}{\partial x} + \frac{1}{Re}\left(\frac{\partial^2 u^*}{\partial x^2} + \frac{\partial^2 u^*}{\partial y^2}\right) \\ &\quad + b_1(x, y)\bar{u}(t) \\ \frac{\partial v^*}{\partial t} + u^*\frac{\partial v^*}{\partial x} + v^*\frac{\partial v^*}{\partial y} &= -\frac{\partial p^*}{\partial y} + \frac{1}{Re}\left(\frac{\partial^2 v^*}{\partial x^2} + \frac{\partial^2 v^*}{\partial y^2}\right) \\ &\quad + b_2(x, y)\bar{u}(t),\end{aligned} \tag{34}$$

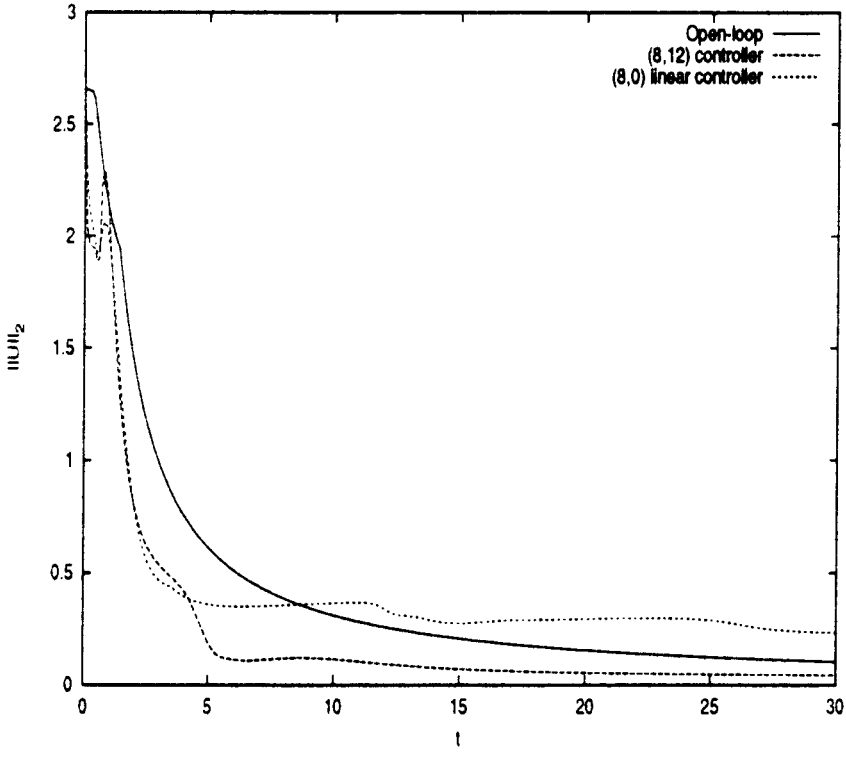

FIG. 4. Profile of energy of open-loop (solid line) and closed-loop system under nonlinear control (dashed line) and linear control (dotted line)—Burgers' equation.

where u^* and v^* are the components of the velocity along the x (parallel to the wall) and y (normal to the wall) axes, respectively, p^* is the pressure, $\bar{u}(t)$ is the vector of manipulated inputs, and $b_1(x, y)$ and $b_1(x, y)$ are the vector distribution functions of the control actuators. We consider the above equations subject to periodic boundary conditions in the x-direction and no-slip boundary conditions on the channel walls. Since we are interested in enhancing the convergence rate to the parabolic base flow, we assume that the flow field and the pressure field can be decomposed into a primary component plus a perturbation,

$$\begin{aligned} u^*(x, y) &= U(y) + u(x, y) \\ v^*(x, y) &= V(x, y) + v(x, y) \\ p^*(x, y) &= P(x, y) + p(x, y), \end{aligned} \tag{35}$$

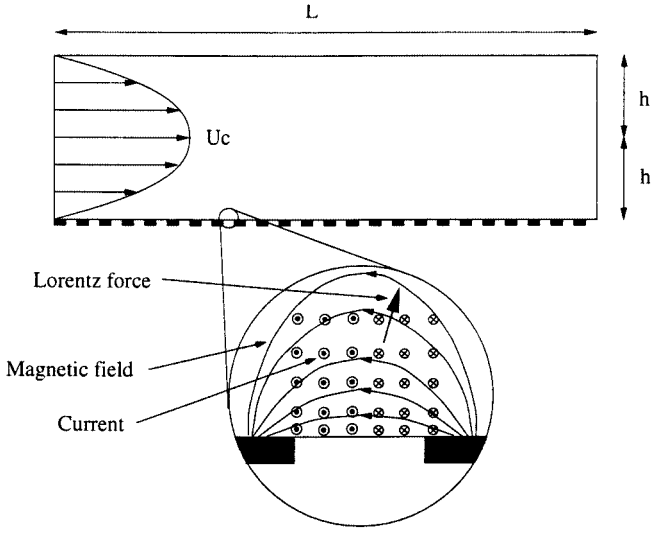

FIG. 5. The 2D channel flow with electromagnetic forcing on the bottom wall.

where u and v are the velocity perturbations in the x and y directions, respectively, and $U(y)$ is a parabolic profile associated with the base channel flow. Also, note that $V(x, y)$, the base velocity field in the normal to the wall direction, is zero, and $P(x, y)$, the base pressure field is such that $\partial P(x, y)/\partial x = constant$ and $\partial P(x, y)/\partial y = 0$. Substituting Eq. (35) into Eq. (34), we obtain

$$\frac{\partial u}{\partial t} + U\frac{\partial u}{\partial x} + u\frac{\partial u}{\partial x} + U'v + v\frac{\partial u}{\partial y} = -\frac{\partial p}{\partial x} + \frac{1}{Re}\left(\frac{\partial^2 u}{\partial x^2} + \frac{\partial^2 u}{\partial y^2} + U''\right) + b_1(x, y)\bar{u}(t) \tag{36}$$

$$\frac{\partial v}{\partial t} + U\frac{\partial v}{\partial x} + u\frac{\partial v}{\partial x} + v\frac{\partial v}{\partial y} = -\frac{\partial p}{\partial y} + \frac{1}{Re}\left(\frac{\partial^2 v}{\partial x^2} + \frac{\partial^2 v}{\partial y^2}\right) + b_2(x, y)\bar{u}(t), \tag{37}$$

where U' and U'' are the first and second-order derivatives of the base flow, $U(y)$, with respect to y. Utilizing the perturbation stream function, ψ, which satisfies

$$u = \frac{\partial \psi}{\partial y}, \qquad v = -\frac{\partial \psi}{\partial x}, \tag{38}$$

Eq. (36) and Eq. (37) can be combined into a single equation for $\psi(x, y, t)$, of the form

$$\left(\frac{\partial}{\partial t} + U\frac{\partial}{\partial x} - \frac{\partial \psi}{\partial x}\frac{\partial}{\partial y} + \frac{\partial \psi}{\partial y}\frac{\partial}{\partial x}\right)\Delta\psi - U''\frac{\partial \psi}{\partial x} = \frac{1}{Re}(\Delta\Delta\psi) + b(x, y)\bar{u}(t), \tag{39}$$

where Δ is the Laplacian in two dimensions and $b(x, y)$ is a nonlinear function whose explicit form is omitted for brevity (note that in the formulation of Eq. (39) the continuity constraint is automatically satisfied). Equation (39) is subjected to the following no-slip boundary conditions on the walls,

$$\begin{aligned} \psi(x, -1, t) &= \psi(x, +1, t) = 0, \\ \frac{\partial \psi}{dy}(x, -1, t) &= \frac{\partial \psi}{dy}(x, +1, t) = 0, \end{aligned} \tag{40}$$

and periodic boundary conditions at $x = 0$ and $x = L$ ($L = 2\pi$ is the length of the domain in the streamwise direction).

To solve the stream function equation using Galerkin's method, we assume that $\psi(x, y, t)$ can be written in the form

$$\psi(x, y, t) = \sum_{n=1}^{N}\sum_{m=0}^{M}\left[a_{nm}(t)\cos(n\alpha_0 x) + b_{nm}(t)\sin(n\alpha_0 x)\right]L_m(y), \tag{41}$$

where $\alpha_0 = 2\pi/L$ is the fundamental wave number and $L_m(y)$ are linear combinations of Chebyshev polynomials, which satisfy the boundary conditions at $y = +1$ and $y = -1$, namely,

$$\begin{aligned} L_m(-1) &= L_m(+1) = 0, \\ \frac{dL_m}{dy}(-1) &= \frac{dL_m}{dy}(+1) = 0. \end{aligned} \tag{42}$$

Using the series expansion of Eq. (41) and Galerkin's method, we reduce the PDE of Eq. (39) into a set of ODEs. The time-integration of the ODEs is performed by using a fourth-order Runge–Kutta scheme. For $Re = 500$ and initial conditions

$$a_{nm} = 0.01, \qquad b_{nm} = 0.01, \qquad n = 1, \ldots, N, m = 0, \ldots, M \tag{43}$$

we found that $N = 8$ and $M = 9$ yield a numerically stable discretization of the PDE system (further increase on N and/or M led to identical simulation results). Under these conditions, Fig. 6 (dashed line) shows the sum of the squares of the modes of the open-loop system ($S = \sum_{n=1}^{N}\sum_{m=0}^{M}(a_{nm}^2(t) + b_{nm}^2(t))$; this quantity is closely related to the energy of the system) which decays to zero.

To enhance the convergence rate to the steady-state, we use the proposed control method to synthesize a nonlinear output feedback controller. Initially, a reduced-order ODE approximation of the PDE of Eq. (39) was obtained via Galerkin's method with $N = 6$ and $M = 9$ and used for controller synthesis. To achieve the control objective, each state of the reduced-order ODE model with $n = 1, 2, 3$ and $m = 0, 1, 2, \ldots, 9$ was considered as a controlled output. To be able to regulate all the outputs, $3 \times 9 \times 2$ control actuators distributing body forces in the near vicinity of the bottom wall by means of Lorenz forces were assumed to be available. The actuator distribution functions are sinusoids in the streamwise direction and decaying exponentials in the normal direction (see [19, 46] for details). A state observer of order $6 \times 9 \times 2$ is used to obtain estimates of all the states used in the controller. Owing to the natural stability of the flow for $Re = 500$, the observer gain, L, was set identically equal to zero. Figure 6 (solid line) shows the profile of S for the nonlinear two-dimensional channel flow under the nonlinear controller. Clearly, the controller significantly enhances the convergence rate of S to zero, compared to the uncontrolled flow (dashed line). Finally, in order to demonstrate the superiority of nonlinear control over linear control, we also implemented on the flow a linear controller obtained by linearizing the nonlinear controller around the steady-state $u(x, y, t) = v(x, y, t) = 0$. The profile of S for the nonlinear two-dimensional channel flow under the linear controller is displayed in Fig. 6 (dotted line).

7. CONCLUSIONS

This paper proposed a methodology for the synthesis of nonlinear finite-dimensional feedback controllers for incompressible Newtonian fluid flows described by two-dimensional Navier–Stokes equations. The controllers are synthesized, using geometric control methods, on the basis of finite-dimensional approximations of the Navier–Stokes equations obtained through combination of Galerkin's method with approximate inertial manifolds. Precise conditions which ensure the stability of the closed-loop system were derived. The method was successfully used to synthesize nonlinear finite-dimensional output feedback controllers for the Burgers' equation and the two-dimensional channel flow that enhance the convergence rates to the spatially uniform steady-state and the parabolic velocity

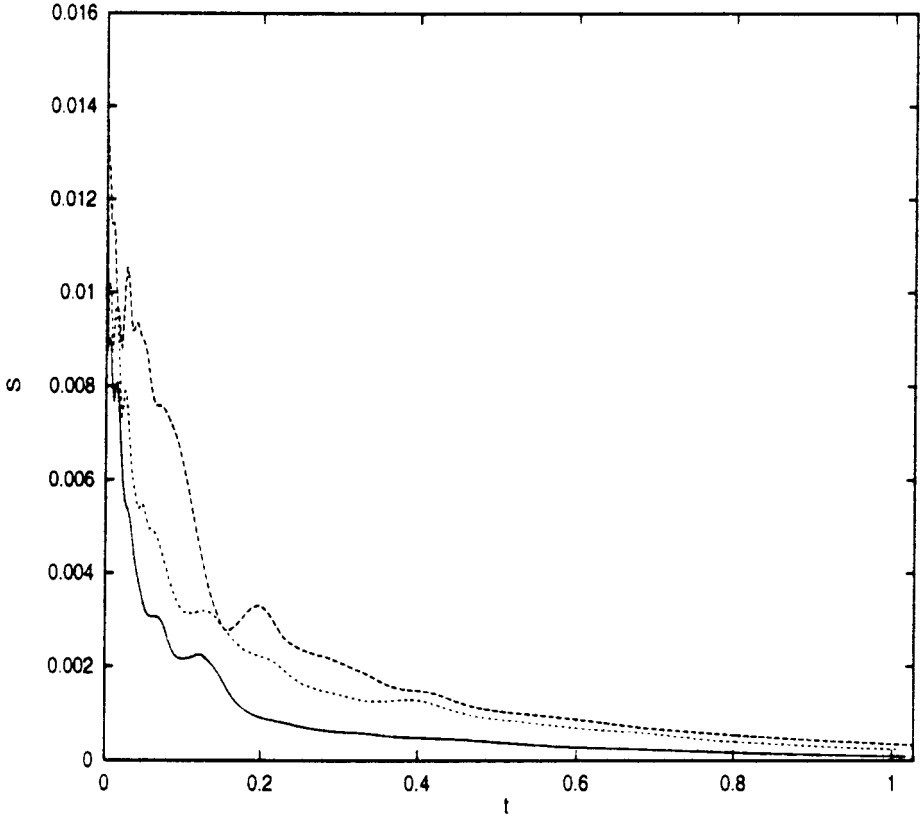

FIG. 6. Profiles of S for open-loop (dashed line) and closed-loop system under nonlinear control (solid line) and linear control (dotted line)—2D channel flow.

profile, respectively. The performance of the proposed controllers was successfully tested through simulations and was shown to be superior to the one of linear controllers.

APPENDIX

Proof of Theorem 1. Under the controller of Eq. (27), the closed-loop system takes the form

$$\frac{d\eta}{dt} = f(\eta) + L(y_m - h_m(\eta)) + g(\eta)\left\{\left[\beta_{1r_1} \cdots \beta_{lr_l}\right]C(\eta)\right\}^{-1}\left\{v - \sum_{i=1}^{l}\sum_{k=0}^{r_i}\beta_{ik}L_f^k h_{ci}(\eta)\right\} \quad (44)$$

$$\dot{x} = \nu\mathscr{A}x + \mathscr{B}\hat{\xi} + \mathscr{R}(x).$$

Applying Galerkin's method to the above system, we obtain

$$\begin{aligned}
\frac{d\eta}{dt} &= f(\eta) + L(y_m - h_m(\eta)) \\
&\quad + g(\eta)\left\{\left[\beta_{1r_1} \cdots \beta_{lr_l}\right]C(\eta)\right\}^{-1}\left\{\upsilon - \sum_{i=1}^{l}\sum_{k=0}^{r_i}\beta_{ik}L_f^k h_{ci}(\eta)\right\} \\
\frac{dx_s}{dt} &= \nu\mathscr{A}_s x_s + \nu\mathscr{A}_{sf}x_f + \mathscr{B}_s\hat{\xi} + \mathscr{R}_s(x_s, x_f) \\
\frac{\partial x_f}{\partial t} &= \nu\mathscr{A}_{fs}x_s + \nu\mathscr{A}_f x_f + \mathscr{B}_f\hat{\xi} + \mathscr{R}_f(x_s, x_f).
\end{aligned} \tag{45}$$

Performing a linearization of the above system around the zero solution, defining the variable $e_o = \eta - x_s$, introducing the fast time-scale $\tau = t/\epsilon$, and setting $\epsilon = 0$, the fast dynamics of the above system are described by the system

$$\frac{de_o}{d\tau} = Ae_o \tag{46}$$

which is clearly exponentially stable (A is a Hurwitz matrix from Assumption 1). Computing the system that describes the slow dynamics of the system of Eq. (45), we obtain

$$\begin{aligned}
\frac{d\xi}{dt} &= \left\{\left[\beta_{1r_1} \cdots \beta_{lr_l}\right]C(\hat{x}_s)\right\}^{-1}\left\{\upsilon - \sum_{i=1}^{l}\sum_{k=0}^{r_i}\beta_{ik}L_f^k h_{ci}(\hat{x}_s)\right\} \\
\frac{dx_s}{dt} &= \nu\mathscr{A}_s x_s + \nu\mathscr{A}_{sf}x_f + \mathscr{B}_s\xi + \mathscr{R}_s(x_s, x_f) \\
\frac{\partial x_f}{\partial t} &= \nu\mathscr{A}_{fs}x_s + \nu\mathscr{A}_f x_f + \mathscr{B}_f\xi + \mathscr{R}_f(x_s, x_f).
\end{aligned} \tag{47}$$

Using the definition $\hat{x}_s = [\xi^T \; x_s^T]^T$, the above system can be written as

$$\begin{aligned}
\frac{d\hat{x}_s}{dt} &= \begin{bmatrix} 0 & 0 \\ \mathscr{B}_s & \nu\mathscr{A}_s \end{bmatrix}\hat{x}_s + \begin{bmatrix} 0 \\ \nu\mathscr{A}_{sf} \end{bmatrix}x_f + \begin{bmatrix} 1 \\ 0 \end{bmatrix}F(\hat{x}_s) + \begin{bmatrix} 0 \\ \mathscr{R}_s(\hat{x}_s, x_f) \end{bmatrix} \\
\frac{\partial x_f}{\partial t} &= \begin{bmatrix} \mathscr{B}_f & \nu\mathscr{A}_{fs} \end{bmatrix}\hat{x}_s + \nu\mathscr{A}_f x_f + \mathscr{R}_f(\hat{x}_s, x_f)
\end{aligned} \tag{48}$$

or equivalently as

$$\begin{aligned}\frac{\partial \hat{x}_s}{dt} &= \hat{\mathscr{A}}_s \hat{x}_s + \hat{\mathscr{A}}_{sf} x_f + \hat{\mathscr{B}}_s F(\hat{x}_s) + \hat{\mathscr{R}}_s(\hat{x}_s, x_f) \\ \frac{\partial x_f}{\partial t} &= \hat{\mathscr{A}}_{fs} \hat{x}_s + \hat{\mathscr{A}}_f x_f + \mathscr{R}_f(\hat{x}_s, x_f),\end{aligned} \tag{49}$$

where the explicit form of the matrices and vector functions used in the above system can be obtained by comparing Eq. (48) with Eq. (49) and is omitted for brevity. On the basis of the above system, when $\dot{x}_f \equiv 0$, assumptions 2 and 3 and the fact that the β_{ik} are chosen so that the roots of the equation $\det(B(s)) = 0$ are in the open left-half of the complex plane, ensure that the resulting system is exponentially stable. To establish stability, when $\dot{x}_f \neq 0$, we compute the linearization of the system of Eq. (49) around the zero solution,

$$\begin{aligned}\frac{d\hat{x}_s}{dt} &= \left(\hat{\mathscr{A}}_s + \hat{\mathscr{B}}_s F\right)\hat{x}_s + \hat{\mathscr{A}}_{sf} x_f \\ \frac{\partial x_f}{\partial t} &= \hat{\mathscr{A}}_{fs} \hat{x}_s + \hat{\mathscr{A}}_f x_f,\end{aligned} \tag{50}$$

where $F\hat{x}_s$ is the linearization of the nonlinear term $F(\hat{x}_s)$ around the origin. Using assumption 4 that the matrix $\left[\begin{smallmatrix} \hat{\mathscr{A}}_s + \hat{\mathscr{B}}_s F & \hat{\mathscr{A}}_{sf} \\ \hat{\mathscr{A}}_{fs} & \hat{\mathscr{A}}_f \end{smallmatrix}\right]$ is stable, we have that the system of Eq. (50) is exponentially stable. Therefore, there exists [42] a real positive number ϵ^* such that $\forall \epsilon \in (0, \epsilon^*]$, the linearization of Eq. (45) is exponentially stable. Using Theorem 5.1.1 in [30], we then have that there exists a real positive number μ such that if $\|x_0\|_2 \leq \mu$, the zero solution of the closed-loop system of Eq. (45) (and thus of Eq. (44)) is exponentially stable.

ACKNOWLEDGMENT

Financial support for this work from a National Science Foundation CAREER award, CTS-9733509, is gratefully acknowledged.

REFERENCES

1. A. Armaou and P. D. Christofides, Wave suppression by nonlinear finite-dimensional control, *Chem. Engrg. Sci.* **55** (2000), 2627–2640.
2. J. Baker and P. D. Christofides, Finite dimensional approximation and control of nonlinear parabolic PDE systems, *Internat. J. Control* **73** (2000), 439–456.

3. P. Bakewell and J. L. Lumley, Viscous sublayer and adjacent wall region in turbulent pipe flow, *Phys. Fluids* **10** (1967), 1880–1889.
4. M. J. Balas, Feedback control of linear diffusion processes, *Internat. J. Control* **29** (1979), 523–533.
5. M. J. Balas, The Galerkin method and feedback control of linear distributed parameter systems, *J. Math. Anal. Appl.* **91** (1983), 527–546.
6. M. J. Balas, Finite-dimensional control of distributed parameter systems by Galerkin approximation of infinite dimensional controllers, *J. Math. Anal. Appl.* **114** (1986), 17–36.
7. A. K. Bangia, P. F. Batcho, I. G. Kevrekidis, and G. E. Karniadakis, Unsteady 2-D flows in complex geometries: Comparative bifurcation studies with global eigenfunction expansion, *SIAM J. Sci. Comput.* **18** (1997), 775–805.
8. S. Beringen, Active control of transition by periodic suction and blowing, *Phys. Fluids* **27** (1984), 1345–1348.
9. J. A. Burns and B. B. King, Optimal sensor location for robust control of distributed parameter systems, *in* "Proceedings, 33rd IEEE Conference on Decision and Control, Orlando, FL, 1994," pp. 3965–3970.
10. J. A. Burns and Y.-R. Ou, Feedback control of the driven cavity problem using LQR designs, *in* "Proceedings, 33rd IEEE Conference on Decision and Control, Orlando, FL, 1994," pp. 289–294.
11. D. M. Bushnell and C. B. McGinley, Turbulence control in wall flows, *Ann. Rev. Fluid Mech.* **21** (1989), 1–20.
12. H. A. Carlson and J. L. Lumley, Active control in the turbulent wall layer of a minimal flow unit, *J. Fluid Mech.* **329** (1996), 341–371.
13. H. Choi, P. Moin, and J. Kim, Active turbulence control for drag reduction in wall-bounded flows, *J. Fluid Mech.* **262** (1994), 75–110.
14. H. Choi, R. Temam, P. Moin, and J. Kim, Feedback control for unsteady flow and its application to the stochastic burger's equation, *J. Fluid Mech.* **253** (1993), 509–543.
15. P. D. Christofides, "Nonlinear and Robust Control of PDE Systems: Methods and Applications to Transport-Reaction Processes," Birkhäuser, Boston, in press.
16. P. D. Christofides and P. Daoutidis, Finite-dimensional control of parabolic PDE systems using approximate inertial manifolds, *J. Math. Anal. Appl.* **216** (1997), 398–420.
17. L. Cortelezzi, K. H. Lee, J. Kim, and J. L. Speyer, Skin-friction drag reduction via reduced-order linear feedback control, *Internat. J. Comput. Fluid Dynam.* **11** (1998), 79–92.
18. L. Cortelezzi and J. L. Speyer, Robust reduced-order controller of laminar boundary layer transition, *Phys. Rev. E* **58** (1998), 1906–1910.
19. C. W. Crawford and G. E. Karniadakis, Reynolds stress analysis of EMHD-controlled wall turbulence. Part I. Streamwise forcing, *Phys. Fluids* **9** (1997), 788–806.
20. A. E. Deane, I. G. Kevrekidis, G. E. Karniadakis, and S. A. Orszag, Low-dimensional models for complex geometry flows: Application to grooved channels and circular cylinders, *Phys. Fluids A* **3** (1991), 2337–2354.
21. M. Desai and K. Ito, Optimal controls of Navier–Stokes equations, *SIAM J. Control Optim.* **32** (1994), 1428–1446.
22. C. Foias, M. S. Jolly, I. G. Kevrekidis, G. R. Sell, and E. S. Titi, On the computation of inertial manifolds, *Phys. Lett. A* **131** (1989), 433–437.
23. C. Foias, G. R. Sell, and E. S. Titi, Exponential tracking and approximation of inertial manifolds for dissipative equations, *J. Dynam. Differential Equations* **1** (1989), 199–244.
24. C. Foias and R. Témam, Algebraic approximation of attractors: The finite dimensional case, *Physica D* **32** (1988), 163–182.

25. K. Fukunaga, "Introduction to Statistical Pattern Recognition," Academic Press, New York, 1990.
26. M. Gad-el-Hak, Flow control, *Appl. Mech. Rev.* **42** (1989), 261–293.
27. M. Gad-el-Hak, Interactive control of turbulent boundary layers: A futuristic overview, *AIAA J.* **32** (1994), 1753–1765.
28. M. Gad-el-Hak and D. M. Bushnell, Separation control, *J. Fluids Engrg.* **113** (1991), 5–30.
29. J. Guckenheimer, Strange attractors in fluids: Another view, *Ann. Rev. Fluid Mech.* **18** (1986), 15–32.
30. D. Henry, "Geometric Theory of Semilinear Parabolic Equations," Springer-Verlag, Berlin/Heidelberg, 1981.
31. P. Holmes, J. L. Lumley, and G. Berkooz, "Turbulence, Coherent Structures, Dynamical Systems and Symmetry," Cambridge Univ. Press, New York, 1996.
32. L. S. Hou and Y. Yan, Dynamics for controlled Navier–Stokes systems with distributed controls, *SIAM J. Control Optim.* **35** (1997), 654–677.
33. A. Isodori, "Nonlinear Control Systems: An Introduction," 2nd ed., Springer-Verlag, Berlin/Heidelberg, 1989.
34. K. Ito and S. S. Ravindran, Optimal control of compressible Navier–Stokes equations, *in* "Proceedings, 35th IEEE Conference on Decision and Control, Kobe, Japan, 1996," pp. 3700–3704.
35. K. Ito and S. S. Ravindran, A reduced order method for control of fluid flows, *in* "Proceedings 35th IEEE Conference on Decision and Control, Kobe, Japan, 1996," pp. 3705–3710.
36. K. Ito and S. S. Ravindran, Reduced order methods for nonlinear infinite dimensional control systems, *in* "Proceedings, 36th IEEE Conference on Decision and Control, San Diego, CA, 1997," pp. 2213–2218.
37. D. A. Jones and E. S. Titi, A remark on quasi-stationary approximate inertial manifolds for the Navier–Stokes equations, *SIAM J. Math. Anal.* **25** (1994), 894–914.
38. S. S. Joshi, J. L. Speyer, and J. Kim, Modeling and control of two dimensional Poiseuille flow, *in* "Proceedings, 34th IEEE Conference on Decision and Control, New Orleans, LA, 1995," pp. 921–927.
39. S. S. Joshi, J. L. Speyer, and J. Kim, A system theory approach to the feedback stabilization of infinitesimal and finite-amplitude disturbances in plane Poiseuille flows, *J. Fluid Mech.* **332** (1997), 157–184.
40. S. Kang and K. Ito, A feedback control law for systems arising in fluid dynamics, *in* "Proceedings, 30th IEEE Conference on Decision and Control, Tampa, AZ, 1992," pp. 384–385.
41. B. B. King and Y. Qu, Nonlinear dynamic compensator design for flow control in a driven cavity, *in* "Proceedings, 34th IEEE Conference on Decision and Control, New Orleans, LA, 1995," pp. 3741–3746.
42. P. V. Kokotovic, H. K. Khalil, and J. O'Reilly, "Singular Perturbations in Control: Analysis and Design," Academic Press, London, 1986.
43. J. L. Lumley, Drag reduction in turbulent flow by polymer additives, *J. Polymer Sci. D Macromol. Rev.* **7** (1973), 263–290.
44. M. Rajaee, S. K. F. Karlsson, and L. Sirovich, Low-dimensional description of free shear flow coherent structures and their dynamical behavior, *J. Fluid Mech.* **258** (1994), 1–20.
45. S. Y. Shvartsman and I. G. Kevrekidis, Nonlinear model reduction for control of distributed parameter systems: A computer assisted study, *AIChE J.* **44** (1998), 1579–1595.
46. S. N. Singh and P. R. Bandyopadhyay, Linear feedback control of boundary layer using electromagnetic microtiles, *Trans. ASME* **119** (1997), 852–858.

47. L. Sirovich, Turbulence and the dynamics of coherent structures. Part I. Coherent structures, *Quart. Appl. Math.* **45** (1987), 561–571.
48. L. Sirovich, Turbulence and the dynamics of coherent structures. Part II. Symmetries and transformations, *Quart. Appl. Math.* **45** (1987), 573–582.
49. L. Sirovich, Turbulence and the dynamics of coherent structures. Part III. Dynamics and scaling, *Quart. Appl. Math.* **45** (1987), 583–590.
50. R. Temam, "Infinite-Dimensional Dynamical Systems in Mechanics and Physics," Springer-Verlag, New York, 1988.
51. E. S. Titi, On approximate inertial manifolds to the Navier–Stokes equations, *J. Math. Anal. Appl.* **149** (1990), 540–557.
52. P. S. Virk, Drag reduction fundamentals, *AIChE J.* **21** (1975), 625–656.